Published in final edited form as:

Eur J Neurosci. 2016 June ; 43(12): 1661–1673. doi:10.1111/ejn.13248.

Amphetamine elevates nucleus accumbens dopamine via an action potential-dependent mechanism that is modulated by endocannabinoids

Dan P. Covey[1], **Kendra D. Bunner**[2], **Douglas R. Schuweiler**[3], **Joseph F. Cheer**[1,4], and **Paul A. Garris**[3]

[1]Department of Anatomy and Neurobiology, University of Maryland School of Medicine, Baltimore, MD, USA

[2]Department of Psychological and Brain Sciences, Indiana University, Bloomington, IN, USA

[3]School of Biological Sciences, Illinois State University, 210 Julian Hall, Normal, IL 61790-4120, USA

[4]Department of Psychiatry, University of Maryland School of Medicine, Baltimore, MD, USA

Abstract

The reinforcing effects of abused drugs are mediated by their ability to elevate nucleus accumbens dopamine. Amphetamine (AMPH) was historically thought to increase dopamine by an action potential-independent, non-exocytotic type of release called efflux, involving reversal of dopamine transporter function and driven by vesicular dopamine depletion. Growing evidence suggests that AMPH also acts by an action potential-dependent mechanism. Indeed, fast-scan cyclic voltammetry demonstrates that AMPH activates dopamine transients, reward-related phasic signals generated by burst firing of dopamine neurons and dependent on intact vesicular dopamine. Not established for AMPH but indicating a shared mechanism, endocannabinoids facilitate this activation of dopamine transients by broad classes of abused drugs. Here, using fast-scan cyclic voltammetry coupled to pharmacological manipulations in awake rats, we investigated the action potential and endocannabinoid dependence of AMPH-induced elevations in nucleus accumbens dopamine. AMPH increased the frequency, amplitude and duration of transients, which were observed riding on top of slower dopamine increases. Surprisingly, silencing dopamine neuron firing abolished all AMPH-induced dopamine elevations, identifying an action potential-dependent origin. Blocking cannabinoid type 1 receptors prevented AMPH from increasing transient frequency, similar to reported effects on other abused drugs, but not from increasing transient duration and inhibiting dopamine uptake. Thus, AMPH elevates nucleus accumbens dopamine by eliciting transients via cannabinoid type 1 receptors and promoting the summation of temporally coincident transients, made more numerous, larger and wider by AMPH. Collectively, these findings are inconsistent with AMPH eliciting action potential-independent dopamine efflux

Correspondence: Paul A. Garris, as above., pagarri@ilstu.edu.

Conflict of interest

None.

and vesicular dopamine depletion, and support endocannabinoids facilitating phasic dopamine signalling as a common action in drug reinforcement.

Keywords

amphetamine; dopamine; endocannabinoids; nucleus accumbens; rat; voltammetry

Introduction

Amphetamine (AMPH) and structurally-related psychostimulants comprise an expansive drug class with broad therapeutic utility and high abuse potential. Prescription AMPH use is indicated for narcolepsy, attention deficit hyperactivity disorder, obesity and traumatic brain injury (Howell & Kimmel, 2008; Bales *et al.*, 2009). AMPH-type psychostimulants also represent the second most widely used illicit drugs worldwide, behind only cannabis but nearly surpassing cocaine and heroin use combined (UNODC, 2014). Despite the pervasive impact and potent addictive properties of this drug class, there remains no accepted or effective pharmacotherapy for AMPH abuse (Forray & Sofuoglu, 2014; Stoops & Rush, 2014). A foundational understanding of AMPH action will greatly aid this important endeavour but, despite extensive effort, a definitive mechanism remains elusive.

The reinforcing effects of abused drugs are mediated by their ability to elevate nucleus accumbens (NAc) dopamine (Di Chiara & Imperato, 1988; Nestler, 2005). Drug mechanisms vary, but AMPH was historically thought to elicit dopamine efflux (Kuczenski, 1983; Seiden *et al.*, 1993; Kuczenski & Segal, 1994; Sulzer, 2011). This action potential-independent, non-exocytotic type of release is mediated by reversal of dopamine transporter function and driven by vesicular dopamine depletion. However, growing evidence also supports an action potential-dependent mechanism for AMPH. Similar to cocaine, nicotine, ethanol, opioids and cannabinoids (Cheer *et al.*, 2004, 2007; Vander Weele *et al.*, 2014), AMPH activates dopamine transients (Ramsson *et al.*, 2011; Covey *et al.*, 2013; Daberkow *et al.*, 2013). These phasic signals generated by burst firing of dopamine neurons (Sombers *et al.*, 2009) are critical to reward-related learning (Steinberg *et al.*, 2014; Hamid *et al.*, 2016) and associated with drug reinforcememnt (Stuber *et al.*, 2005). Although not established for AMPH but indicating a shared mechanism, blocking cannabinoid type 1 (CB1) receptors suppresses transient activation by broad classes of abused drugs (Cheer *et al.*, 2004, 2007). Moreover, CB1 receptors on afferent GABAergic terminals in the ventral tegmental area (VTA) shape NAc dopamine signalling by disinhibiting dopamine neurons to facilitate their burst firing (Matyas *et al.*, 2008; Wang *et al.*, 2015). Disrupting this process thus represents an emerging pharmacotherapeutic target for addiction treatment (Lupica & Riegel, 2005; Parsons & Hurd, 2015). Because dopamine transients also depend on intact vesicular dopamine (Owesson-White *et al.*, 2012), their activation by AMPH via an endocannabionoid mechanism is ostensibly incompatible with AMPH depleting vesicular dopamine and driving efflux.

Here we used fast-scan cyclic voltammetry (FSCV) in awake rats to investigate the action potential and endocannabinoid dependence of AMPH-induced elevations in NAc dopamine.

AMPH robustly increased the frequency, amplitude and duration of dopamine transients, which were observed riding on top of slower dopamine increases. Suprisingly, silencing dopamine neuron firing abolished all dopamine elevations with AMPH, identifying an action potential-dependent origin. Blocking CB1 receptors prevented AMPH from increasing transient frequency but not duration and inhibiting dopamine uptake. Thus, AMPH elevates NAc dopamine by promoting the temporal summing of dopamine transients, made more numerous, larger and wider by AMPH. Inconsistent with dopamine efflux and vesicular dopamine depletion, these results support endocannabinoids facilitating the AMPH-induced activation of dopamine transients.

Materials and methods

Animals

Male Sprague Dawley rats (300–400 g) (Harlan, Indianapolis, IN, USA) were housed in a temperature-controlled room maintained on a reverse 12 h light/dark cycle and allowed access to food and water *ad libitum*. Rats were housed individually following surgery. Animal care and experimental procedures conformed to the National Institutes of Health *Guide for the Care and Use of Laboratory Animals* and were approved by the Institutional Animal Use and Care Committees at Illinois State University.

Carbon-fibre microelectrodes

Individual carbon fibres (r = 3.5 μm; Hexcel Corporation) were pulled (micropipette puller, Narishige) in glass capillary tubes (Sutter Instruments). The seal between the glass and carbon fibre was reinforced with epoxy (Miller-Stephenson), and the exposed fibre was cut to ~80–100 μm in length.

Surgery

Rats were anaesthetized with ketamine (80 mg/kg, i.p.) and xylazine (20 mg/kg, i.p.) and implanted with a chronic indwelling Silastic® cannula (0.012 inches inner diameter and 0.025 inches outer diameter) into the right jugular vein (Calipari *et al.*, 2013). The cannula exited the skin on the dorsal surface in the region of the scapulas. Immediately following catheterization, rats were immobilized in a stereotaxic frame and surgically prepared for freely moving FSCV recording as described previously (Aragona *et al.*, 2008; Sombers *et al.*, 2009). A guide cannula (Bioanalytical Systems) for housing the microdrive for the carbon-fibre microelectrode was positioned above the NAc shell (+1.7 mm anterior, +0.8 mm lateral, −2.5 mm ventral relative to bregma) (Paxinos & Watson, 1998), and a combination bipolar stimulating electrode/guide cannula (26 gauge; Plastics One) was implanted ipsilaterally targeting the VTA (+5.4 mm posterior, +1.2 mm lateral, −7.8 mm ventral) at a 6° angle. An Ag/AgCl reference electrode was placed in the contralateral cortex. All components were permanently affixed with dental cement.

Recording sessions

After recovery from surgery, FSCV was used to monitor extracellular dopamine by applying a triangular waveform (−0.4 to +1.3 V at 400 V/s) at 10 Hz to the implanted carbon-fibre microelectrode. Naturally occurring, drug-evoked and electrically evoked (biphasic; 2 ms/

phase, 24 pulses, 60 Hz, ±125 μA) dopamine changes were recorded before and throughout the experimental session. Electrically evoked recordings verified the performance of the carbon-fibre microelectrode and permitted a training set to be recorded for principal component regression, in order to statistically extract the dopamine component from the mixed-analyte FSCV recording (Heien *et al.*, 2005). Dopamine transients were analysed for amplitude (peak), duration (width at half-maximal amplitude) and frequency (inverse of inter-transient interval) using Mini Analysis (Synaptosoft, Decatur, GA, USA). Electrically evoked dopamine signals were characterized by maximal amplitude and the rate of dopamine uptake using a first-order rate constant (k) with Demon Analysis Software (Yorgason *et al.*, 2011). After the experiment, the carbon-fibre microelectrode was calibrated as described previously (Covey *et al.*, 2013). The recording site was verified in the NAc by passing direct current (~100 μA) for 20 s through a stainless-steel electrode, inserted to the same position as the carbon-fibre microelectrode. Animals were anaesthetized with urethane (1.5 g/kg, i.p.) and decapitated, and the brain removed for histology. Brains were post-fixed in 4% paraformaldehyde in phosphate-buffered saline and then placed in 10% sucrose solution in phosphate-buffered saline for 48 h followed by 30% sucrose solution in phosphate-buffered saline for 48 h. Coronal sections (60 μm) were mounted and stained with cresyl violet.

Ventral tegmental area microinfusions

Microinfusions were made through a guide cannula attached to the bipolar stimulating electrode (Plastics One) targeting the VTA. An injection cannula was inserted into the guide cannula ending 1 mm above the tip of the stimulating electrode (Plastics One); the injection cannula was cut to extend 1 mm beyond the guide cannula tip. Tetrodotoxin (TTX) or artificial cerebrospinal fluid (aCSF) was infused using a syringe pump (Harvard Apparatus) with a flow rate of 0.5 μL/min over a 1 min period. The injection cannula was left in place for 2 min to allow diffusion.

Experimental design

Two between-subjects designs were used. For the experiment assessing the effects of TTX, used to inhibit action potentials, following a 15 min baseline recording period, all animals received either TTX (10 μM) or aCSF infused into the VTA, followed 15 min later by intravenously administered saline. A 1 mg/kg dose of AMPH was intravenously administered 15 min later. For the experiment assessing the effects of rimonabant (RIMO) (SR141716A), a CB1 receptor antagonist/inverse agonist, following a 15 min baseline recording period, RIMO (0.3 mg/kg) or vehicle (VEH) was administered intravenously, followed 4.5 min later by AMPH (1 mg/kg) also administered intravenously. This design was based on previous work with RIMO and dopamine transients (Cheer *et al.*, 2007). All drugs administered intravenously were injected in 0.5 mL over 10 s. After each recording period, electrical stimulation was applied to the VTA to assess treatment effects on the pre-synaptic regulation of NAc dopamine release.

Statistics

Characteristics of dopamine transients and electrically evoked dopamine signals were compared using two-way repeated-measures ANOVA with SIGMAPLOT (version 12.5).

Holm–Sidak *post hoc* tests were used for planned and unplanned comparisons of group- and time-dependent effects. Averaged changes in AMPH-evoked dopamine concentration following RIMO vs. VEH were compared using a Student's *t*-test. Path analysis was conducted using SAS version 9.3 (SAS Institute) to assess the direct and indirect effects of AMPH and RIMO on transient frequency, amplitude and duration. Path coefficients were statistically compared using 95% confidence intervals. Models were compared using Akaike information criteria, reflecting the information lost by using models to describe data in path analysis (Anderson, 2008). Unless noted otherwise, data are expressed as mean ± SEM and statistical significance was set at $P < 0.05$.

Drugs

The D-AMPH hydrochloride (Sigma-Aldrich, St Louis, MO, USA) was dissolved in saline (0.9%). TTX was dissolved in aCSF. RIMO (Research Triangle Institute–National Institute on Drug Abuse, Raleigh, NC, USA) was freshly suspended in a 1 : 1 : 18 ratio of ethanol, emulphor (Alkamuls EL-620; Rhodia, Cranbury, NJ, USA) and saline (0.9%).

Results

Amphetamine elevates nucleus accumbens dopamine measured by fast-scan cyclic voltammetry

Freely moving rats were placed in a behavioural chamber and the FSCV microsensor, a carbon-fibre microelectrode, was lowered into the NAc to a site exhibiting spontaneously occurring dopamine transients (> 2/min). As shown in Fig. 1, extracellular dopamine changes were then quantified with 100 ms resolution by FSCV in 90 s sampling windows beginning 10 s before drug infusion. FSCV uses a voltammogram, the relationship between measured current and applied potential, to identify the analyte detected (Robinson *et al.*, 2008). Voltammograms were plotted sequentially in time using false colour (Michael *et al.*, 1999), shown underneath dopamine recordings. Individual dopamine voltammograms (insets) were characterized by an oxidative peak around +0.65 V on the forward sweep and a reductive peak around −0.2 V on the reverse sweep, similar to literature values (Heien *et al.*, 2003). Monitoring current at the oxidative peak potential in successive voltammograms (horizontal white dashed line on colour plots) revealed the time-dependent dopamine record after conversion to concentration using post-calibration. Principal component regression further resolved dopamine from other analytes in the complex FSCV record (Heien *et al.*, 2005).

Representative dopamine responses are shown for intravenously administered saline (Fig. 1A) and AMPH (Fig. 1B). During the saline recording, infrequent small changes were observed in the relatively flat dopamine record, reflecting spontaneously occurring dopamine transients. Following AMPH administration, larger dopamine transients were seen riding on top of a slower tonic dopamine increase that potentially reflects dopamine efflux. Individual transients and the source of frequency, amplitude and duration metrics are highlighted by dashed boxes. Similar effects have been described for intraperitoneally administered AMPH (Ramsson *et al.*, 2011; Covey *et al.*, 2013; Daberkow *et al.*, 2013), although dopamine changes were smaller and were initiated much later in time (> 90 s). The

faster onset of dopamine changes reported here, within a few seconds, is consistent with AMPH effects on dopamine neuron firing and behaviour after intravenous adminstration (Bunney *et al.*, 1973; Browman *et al.*, 1998; Milesi-Hallé *et al.*, 2007) and FSCV-measured dopamine changes elicited by other abused drugs administered intravenously (Cheer *et al.*, 2004, 2007; Aragona *et al.*, 2008; Vander Weele *et al.*, 2014). The overall goal of the present study was to resolve the contributions of dopamine efflux and transients to AMPH-induced elevations in NAc dopamine.

Silencing dopamine neuron firing abolishes amphetamine-induced elevations in nucleus accumbens dopamine

We resolved action potential-dependent and -independent effects of AMPH by inactivating impulse flow to the NAc using TTX infusions into the VTA. The efficacy of TTX was initially assessed. For this experiment, an electrically evoked dopamine recording was collected (Pre) and then either TTX or aCSF as a control was infused followed by a second evoked recording. TTX and aCSF therefore comprised the group factor, and stimulation was the time-dependent, repeated-measures factor. Consistent with silencing dopamine neuron firing, representative recordings demonstrated that TTX caused a rapid drop in basal dopamine (Fig. 2A) and abolished dopamine signals electrically evoked by a stimulating electrode attached to the infusion cannula (Fig. 2B, bottom panel). Selected stimulus parameters, which are reinforcing in the paradigm of intracranial self-stimulation (Cheer *et al.*, 2005), evoked dopamine signals resembling naturally occuring dopamine transients. In contrast, a control infusion of aCSF did not alter the evoked signal (Fig. 2B, top panel). Averaged results quantifying the maximal amplitude of electrically evoked dopamine signals ($[DA]_{Stim}$) were consistent (Fig. 2C), and statistical analysis demonstrated a significant group × stimulation interaction ($F_{1,7} = 7.7$, $P = 0.028$). TTX, but not aCSF, significantly ($P = 0.005$) decreased $[DA]_{Stim}$ and completely eliminated this measure of action potential-dependent dopamine signalling.

The effects of TTX on spontaneously occurring dopamine transients and AMPH-induced elevations in NAc dopamine were assessed between stimulations. For transient measures, TTX and aCSF represented the group factor, but four treatments delivered successively in time comprised the repeated measure. Dopamine transients were recorded during each treatment. Baseline activity was recorded initially in both goups during the first treatment (Pre). Either TTX or aCSF was infused into the VTA during the second treatment (intracranial). Saline was adminsistered intravenously in both groups during the the third treatment. Finally, AMPH was administered intravenously in both groups during the fourth treatment (AMPH). Representative recordings shown in Fig. 3A and B demonstrate that TTX infused into the VTA prevented all AMPH-induced dopamine elevations. Averaged results obtained from the analysis of dopamine transients are shown in Fig. 3C. For frequency data shown in the top panel, there was a significant effect of group ($F_{1,24} = 84.93$, $P < 0.001$), treatment ($F_{3,24} = 16.36$, $P < 0.001$) and a significant group × treatment interaction ($F_{3,24} = 23.51$, $P < 0.001$). For amplitude data in the middle panel, there was a significant effect of group ($F_{1,24} = 17.62$, $P = 0.003$) and treatment ($F_{3,24} = 10.80$, $P < 0.001$), and a significant group × treatment ($F_{3,24} = 25.19$, $P < 0.001$). For duration data in the bottom panel, there was a significant effect of group ($F_{1,24} = 157.86$, $P < 0.001$) and

treatment ($F_{3,24}$ = 22.35, P < 0.001), and a significant group × treatment ($F_{3,24}$ = 47.30, P < 0.001).

Consistent with intraperitoneal administration (Covey *et al.*, 2013; Daberkow *et al.*, 2013), AMPH significantly (P < 0.001) increased transient frequency, amplitude and duration relative to baseline (Pre). These AMPH-induced increases in transient characteristics were significantly (P < 0.001) decreased by TTX, which completely prevented AMPH from eliciting dopamine transients. TTX also significantly (P < 0.001) decreased all measures of spontaneously occurring dopamine transients and completely eliminated these phasic signals. By contrast, transient measures recorded during aCSF delivered intracranially and saline delivered intravenously were not significantly different compared with those recorded during baseline (Pre). Baseline transients were also not significantly different between groups. Taken together, these results demonstrated that TTX infused into the VTA completely eliminated ongoing and AMPH-evoked phasic dopamine signalling in the NAc.

The effects of TTX on averaged dopamine elevations in the NAc were also assessed. This measure may comprise multiple aspects of dopamine signalling, e.g. tonic, phasic and action potential-independent (efflux), and therefore provides broader insight into observed dopamine changes. As shown in Fig. 4A, AMPH elicited a rapid increase in averaged dopamine concentration that began to plateau around 40 s. In contrast, TTX completely eliminated AMPH-induced dopamine elevations. Individual dopamine transients were not observed in the aCSF response due to averaging, which masked transients that occurred asynchronously across animals. To assess group effects of AMPH and TTX across a longer time span, the change in dopamine concentration (Δ[DA]) was calculated for each 90 s epoch, averaged across animals and plotted against time for 15 min. This time span is suitable for observing the effects of intravenously administered AMPH on dopamine neuron firing and behaviour (Bunney *et al.*, 1973; Browman *et al.*, 1998; Milesi-Hallé *et al.*, 2007), AMPH-induced dopamine efflux measured by FSCV in striatal slices (Iravani & Kruk, 1995; Jones *et al.*, 1998; Schmitz *et al.*, 2001; Patel *et al.*, 2003) and increases in tonic dopamine measured in the striatum by FSCV following intraperitoneal administration of AMPH (Ramsson *et al.*, 2011; Covey *et al.*, 2013; Daberkow *et al.*, 2013). Plotting Δ[DA] within each 90 s epoch also did not violate principle component regression, which breaks down over prolonged, continuous time periods (Heien *et al.*, 2005; Hermans *et al.*, 2008). As shown in Fig. 4B, AMPH elicited an increase in Δ[DA] only in the first epoch, and TTX completely eliminated this increase. Statistical analysis demonstrated a significant group × time interaction ($F_{27,153}$ = 3.62, P = 0.011). AMPH also significantly (P < 0.001) increased Δ[DA] in the first 90 s epoch following aCSF treatment relative to all other epochs, although no other significant differences were found between any other epochs in the TTX and aCSF groups. Taken together, these results are consistent with efflux-insensitive and action potential-dependent actions of AMPH.

These results also underscore the suitability of the experimental design. For example, aCSF injection into the VTA and intravenously administered saline indicated that these control manipulations did not alter dopamine neuron function and highlighted the stability of measuring dopamine transients by FSCV. In addition, the complete elimination of electrically evoked dopamine signals and spontaneously occurring dopamine transients by

TTX was also critical. Indeed, because VTA infusion of either lidocaine or the glutamate receptor antagonist, (2R)-amino-5-phosphonopentanoate (AP-5), does not abolish electrically evoked dopamine signals or spontaneously occurring and cocaine-induced dopamine transients (Sombers *et al.*, 2009; Owesson-White *et al.*, 2012), residual action potential-dependent signalling would complicate the assessment of AMPH-induced dopamine efflux using these manipulations. With TTX, by contrast, such a residual increase in response to AMPH would be considered evidence for efflux, because this manipulation completely abolished action potential-dependent signalling.

Blockade of cannabinoid type 1 receptors diminishes amphetamine-induced elevations in nucleus accumbens dopamine but does not alter pre-synaptic dopamine function

We used the CB1 receptor antagonist/inverse agonist, RIMO, to examine whether endocannabinoids mediate AMPH-induced elevations in NAc dopamine. For this experiment, separate groups received either VEH or RIMO, and three treatments delivered successively in time comprised the repeated measure. Baseline transient activity was recorded initially in both groups during the first treatment (Pre). Either RIMO or VEH was administered intravenously during the second treatment (VEH/RIMO). Finally, AMPH was administered intravenously in both groups during the third treatment (AMPH). As shown by representative recordings in Fig. 5, RIMO markedly reduced the ability of AMPH to elevate NAc dopamine. In particular, the tonic dopamine increase appeared suppressed, as did the frequency of transients, compared with VEH. Statistical analysis of transient characteristics (RIMO, $n = 6$; VEH, $n = 5$) demonstrated a significant main effect of treatment on frequency (Fig. 5C, top panel) ($F_{2,8} = 5.07$, $P = 0.03$), amplitude (Fig. 5C, middle panel) ($F_{2,8} = 16.93$, $P = 0.001$) and duration (Fig. 5C, bottom panel) ($F_{2,8} = 48.08$, $P < 0.001$). Planned comparisons demonstrated that AMPH significantly (all $P < 0.01$) increased frequency, amplitude and duration (see Fig. 5 legend for details). However, indicating differential effects on transient characteristics, RIMO prevented AMPH from significantly increasing frequency (AMPH vs. Pre, $P = 0.67$; AMPH vs. RIMO, $P = 0.63$) and amplitude (AMPH vs. Pre, $P = 0.44$; AMPH vs. RIMO, $P = 0.24$), but not duration (AMPH vs. Pre, $P = 0.001$; AMPH vs. RIMO, $P < 0.001$). No significant ($P = 0.53$–0.93) effects of VEH or RIMO were observed relative to baseline (Pre) for any transient characteristic, suggesting that RIMO did not alter ongoing dopamine neuron function. As shown in Fig. 6A, RIMO also attenuated AMPH-induced elevations in averaged dopamine concentration. Statistical analysis of the maximal change in dopamine concentration ($[DA]_{Max}$) calculated in each animal across this 90 s epoch and shown in Fig. 6B demonstrated that RIMO caused a significant decrease in this measure relative to VEH (196 ± 3.2 and 441 ± 9.6 nM, respectively; $t_8 = 2.37$, $P = 0.02$).

To assess whether RIMO was acting pre-synaptically on dopamine terminals, its effects on dopamine signals electrically evoked by stimulation of the VTA were measured before and after intravenous AMPH administration. These measurements, shown in Fig. 7, were collected in the same experiment described in Fig. 5 and, thus, group and treatment factors were identical. Although neither VEH (Fig. 7A) nor RIMO (Fig. 7B) altered electrically evoked dopamine signals, AMPH elicited a robust and similar increase in both groups. The maximal concentration of electrically evoked dopamine ($[DA]_{Stim}$) was calculated from these recordings, and averaged values plotted in Fig. 7C showed similar effects. Statistical

analysis demonstrated a significant main effect of treatment on $[DA]_{Stim}$ ($F_{2,16} = 11.147$, $P < 0.001$), and planned comparisons demonstrated that AMPH significantly ($P < 0.001$) increased $[DA]_{Stim}$ in both the VEH and RIMO groups (see Fig. 7 legend for details). Although not assessed here, the AMPH-induced increase in $[DA]_{Stim}$ has previously been shown to be primarily mediated by an increase in exocytotic dopamine release measured *in vivo* by FSCV (Ramsson *et al.*, 2011; Avelar *et al.*, 2013; Covey *et al.*, 2013; Daberkow *et al.*, 2013). Compared with baseline, pre-AMPH $[DA]_{Stim}$ was not significantly changed by RIMO ($P = 0.80$) or VEH ($P = 0.73$). Similar results were found for dopamine uptake (Fig. 7D), calculated as a first-order rate constant (k) from the descending portion of the electrically evoked dopamine signal. Statistical analysis demonstrated a significant main effect of treatment ($F_{2,16} = 19.76$, $P < 0.001$), and planned comparisons demonstrated that AMPH significantly (all $P < 0.01$) decreased k in both the VEH and RIMO groups (see Fig. 7 legend for details). These results are consistent with previous work demonstrating an inhibition of dopamine uptake by AMPH also measured *in vivo* by FSCV (*vide supra*). Compared with baseline, pre-AMPH k was not significantly different compared with RIMO ($P = 0.87$) or VEH ($P = 0.62$). Taken together, these results suggested that AMPH increased exocytotic dopamine release and decreased dopamine uptake in the NAc, and that RIMO did not alter these pre-synaptic AMPH actions.

Amphetamine directly and independently increases the frequency and amplitude of dopamine transients

Complex drug effects and the potential interplay between measures of dopamine transients hinders a mechanistic determination of psychostimulant-induced increases in transient frequency, amplitude and duration (Shi *et al.*, 2000, 2004; Stuber *et al.*, 2005; Wightman *et al.*, 2007; Aragona *et al.*, 2008; Daberkow *et al.*, 2013; for review, see Covey *et al.*, 2014). For example, increased frequency has been attributed to both enhanced burst firing of dopamine neurons and increased amplitude, which in theory could increase the number of dopamine transients rising above the detection limit for FSCV. Increased amplitude, in turn, has been attributed to increased exocytotic dopamine release, enhanced intraburst properties (i.e. number and frequency of action potentials within a burst) of dopamine neurons and decreased dopamine uptake. Whereas increased duration has been linked to inhibited dopamine uptake, transients of different amplitudes could exhibit different durations. We therefore used path analysis to further resolve the activation of dopamine transients by AMPH and its modification by RIMO. Path analysis (Mitchell, 2001) assesses the effects of multiple independent variables on a dependent variable, but also allows for the possibility that variables can interact and thereby function as both dependent and independent variables. Path coefficients, the output of path analysis, are standardized regression coefficients indicating strength (i.e. maximum of 1) and direction (i.e. positive or negative) of causal relationships between variables.

Figure 8A shows four models that were assessed by path analysis. Arrows demarcate direct relationships between variables tested in the model. Significant path coefficients are shown above each arrow and the Akaike information criteria score (the higher the value, the less data described by the model) is provided below each model. The most favourable model based on Akaike information criteria score (top left) indicated significant ($P < 0.0001$) direct

effects of AMPH on frequency, amplitude and duration, but no significant differences in the strength of these effects. These results are consistent with AMPH-induced increases in transient characteristics shown in Figs 3C and 5C, and demonstrated by ANOVA. The second most favourable model (bottom right) found similar direct effects ($P < 0.0001$) in addition to a significant ($P < 0.0001$) direct effect of amplitude on duration, indicating that larger amplitude transients exhibited longer durations. No significant differences were found in the strength of these effects. However, none of the models demonstrated a significant direct effect of amplitude on frequency, indicating that AMPH increased transient frequency independent of increasing amplitude. A significant direct effect of duration on amplitude was also not found, indicating that AMPH increased transient amplitude independent of increasing duration. Taken together, these results are consistent with AMPH: (i) increasing transient frequency by activating burst firing of dopamine neurons but not by increasing transient amplitude; (ii) increasing transient amplitude by increasing exocytotic dopamine release and intraburst properties but not by increasing transient duration; and (iii) increasing transient duration by inhibiting dopamine uptake and increasing transient amplitude.

The same four models were assessed by path analysis to further evaluate how RIMO modified the activation of dopamine transients by AMPH. Figure 8B shows the two most favourable models based on Akaike information criteria score. Consistent with the effects of RIMO on the AMPH-induced activation of dopamine transients shown in Fig. 5C and analysed by ANOVA, both models demonstrated a significant (left, $P = 0.0002$; right, $P = 0.0044$) direct effect of AMPH on duration but not on frequency or amplitude in the presence of RIMO. The most favourable model (right) also found a significant ($P < 0.0001$) direct effect of amplitude on duration, consistent with the path analysis shown in Fig. 8A. Also consistent with this previous path analysis, none of the models found significant direct effects of amplitude on frequency or duration on amplitude. Taken together, these results are consistent with RIMO preventing the AMPH-induced increase in transient frequency by preventing the activation of burst firing by dopamine neurons. RIMO preventing the increase in transient amplitude, but sparing the increase in electrically evoked dopamine signals with AMPH, suggests that AMPH increases transient amplitude by enhancing intraburst properties of dopamine neurons but not by increasing exocytotic dopamine release. However, although non-significant, there was a trend for increased transient amplitude with RIMO, suggesting the possibility that both mechanisms were involved. Moreover, the independence of duration from amplitude, observed with both RIMO and VEH (above), suggests that these increases in transient amplitude were not due to AMPH inhibiting dopamine uptake. Finally, the sparing of AMPH-induced dopamine uptake inhibition (Fig. 7C) and increases in transient duration, coupled with no change in baseline transient activity, with RIMO suggest that residual AMPH-induced elevations in NAc dopamine after CB1 receptor blockade (Fig. 6) were mediated, at least in part, by an increase in the summation of extant dopamine transients, now wider due to slowed uptake.

Discussion

Here we investigate the action potential and endocannabinoid dependence of AMPH-induced elevations in NAc dopamine. Our results identify AMPH actions inconsistent with

action potential-independent dopamine efflux and vesicular dopamine depletion but dominated by an endocannabinoid-mediated activation of dopamine transients.

Dopamine efflux and action potential-independent dopamine signalling

We show that AMPH, delivered at a 1 mg/kg dose supporting self-administration (Pickens & Harris, 1968; Yokel & Pickens, 1973), elicited dopamine transients in the NAc riding on top of tonic dopamine increases. Because reinforcing effects of abused drugs are mediated by their ability to elevate NAc dopamine (Di Chiara & Imperato, 1988; Nestler, 2005) and because cocaine self-administration is associated with transient activation in this ventral striatal region (Stuber *et al.*, 2005), observed dopamine changes may relate to AMPH reinforcement. Transient activation and tonic dopamine increases have previously been recorded *in vivo* following intraperitoneal AMPH administration (Ramsson *et al.*, 2011; Covey *et al.*, 2013; Daberkow *et al.*, 2013), although the origin of the slower dopamine changes was not established. To resolve the action potential-independent contributions of AMPH to elevations in NAc dopamine, we infused TTX onto dopamine cell bodies. Surprisingly, TTX abolished all AMPH-induced dopamine elevations, identifying an action potential-dependent origin. The observed transient activation is thus consistent with AMPH enhancing burst firing of dopamine neurons and acting pre-synpatically at dopamine terminals to increase exocytotic dopamine release and inhibit dopamine uptake (Covey *et al.*, 2013, 2014; Daberkow *et al.*, 2013). However, the underlying cause of tonic dopamine increases remains unknown.

Our evidence suggests overlapping transients, but AMPH increasing tonic dopamine neuron firing and altering circuits indirectly controlling NAc dopamine (Howell & Kimmel, 2008) are other possibilities. Our inability to detect AMPH-induced dopamine increases after TTX is in contrast with the considerable body of work obtained from reduced preparations (Sulzer *et al.*, 2005) and *in vivo* microdialysis (Kuczenski & Segal, 1994), which have defined AMPH action as action potential independent and non-exocytotic. We do not at this time have an explanation for this discrepancy. The use of FSCV in the present study does not appear to be limiting, because this microsensor technique has demonstrated dopamine efflux in slices (Jones *et al.*, 1998; Schmitz *et al.*, 2001; Patel *et al.*, 2003). Other differences must therefore account for FSCV demonstrating micromolar efflux *in vitro*, but no efflux above nanomolar detection limits *in vivo*. AMPH is thought to deplete vesicular dopamine thereby increasing cytosolic dopamine, which is released from the neuron via reversal of dopamine transporter function (Seiden *et al.*, 1993; Sulzer *et al.*, 2005). Consistent with this action, AMPH-induced efflux tracks robust decreases in electrically evoked dopamine signals in slices (*vide supra*). However, AMPH augments these signals *in vivo*, even at high doses (20 mg/kg), suggesting that the readily releasable pool is intact or even enhanced (present study; Ramsson *et al.*, 2011; Daberkow *et al.*, 2013; Avelar *et al.*, 2013; Covey *et al.*, 2013). Discrepancies between the two preparations could be a matter of AMPH dose (Schmitz *et al.*, 2001; Siciliano *et al.*, 2014). However, other factors are probably involved, because AMPH actions also differ within preparations, e.g. (i) AMPH when delivered by pressure ejection in slices can increase electrically evoked dopamine signals (Iravani & Kruk, 1995) but decreases these signals when delivered in superfusion; (ii) AMPH decreases electrically evoked signals *in vivo* when evoked by long-duration trains but increases these signals when

evoked by short-duration trains (Covey *et al.*, 2013); and (iii) AMPH administered *in vivo* within a dose range activating dopamine transients partially depletes dopamine vesicular content as analysed *ex vivo* in isolated vesicles (Omiatek *et al.*, 2010). Clearly, more work is needed to clarify this multitude of AMPH actions.

Analytical differences may account for discrepancies reported for *in vivo* AMPH actions. Microdialysis lacks the temporal resolution to monitor real-time dopamine changes (Robinson *et al.*, 2008), which precludes comparison of effects on fast signals readily measured by FSCV. Technical advances have more recently brought tonic dopamine changes within the realm of FSCV (Heien *et al.*, 2005) and permit comparisons. Whereas AMPH robustly increases dialysate dopamine up to ~30-fold (Kuczenski *et al.*, 1991, 1997), FSCV has identified typically no or relatively small (< 100 nM) increases with equivalent dosing (Wiedemann *et al.*, 1990; Ramsson *et al.*, 2011; Covey *et al.*, 2013; Daberkow *et al.*, 2013). Discrepancies have been attributed to the large dialysis probe damaging tissue and altering dopamine signalling at the sampling site, compared with the minimal implantation damage caused by the ~50-fold smaller microsensor (Ramsson *et al.*, 2011; Jaquins-Gerstl & Michael, 2015). Although probe–tissue interactions have yet to be fully characterized, similar phenomena may contribute to microdialysis (Westerink *et al.*, 1987; Nomikos *et al.*, 1990; Benwell *et al.*, 1993), but not FSCV, demonstrating TTX-insensitive dopamine increases with AMPH. However, TTX-sensitive increases in NAc dialysate dopamine with AMPH have been reported in mice with the C57BL/6L but not the DBA/2J background (Ventura *et al.*, 2004), suggesting that other factors are involved.

It should also be emphasized that effects of only one intravenous dose, acutely administered non-contingently, was examined in the NAc. Thus, AMPH may elicit efflux by other dosing regimens and in other regions. Although established in the dorsal striatum, efflux is less studied in the NAc and distinct AMPH effects potentially render the dorsal striatum more susceptible (Avelar *et al.*, 2013; Covey *et al.*, 2013). It seems unlikely that TTX prevented AMPH from interacting with the dopamine transporter and reversing its function. First, TTX was infused into the VTA, whereas efflux was assessed in the NAc, and diffusion over this distance of several mm is prohibitive (Aragona *et al.*, 2008; Freund *et al.*, 2010). Second, efflux has been observed with TTX applied directly to dopamine terminals (Bowyer *et al.*, 1987; Westerink *et al.*, 1987; Nomikos *et al.*, 1990; Benwell *et al.*, 1993). Third, efflux has been demonstrated in slices (Iravani & Kruk, 1995; Jones *et al.*, 1998; Schmitz *et al.*, 2001; Patel *et al.*, 2003) and synaptosomes (Fischer & Cho, 1979; Bowyer *et al.*, 1987), suggesting that dopamine cell body input to terminals, which would be blocked by TTX, is unnecessary for this AMPH action. Consistent with this conclusion is that TTX applied to the medial forebrain bundle does not alter glutamate-induced dopamine efflux measured in the striatum by FSCV (Borland & Michael, 2004). Like AMPH, the glutamate agonist, *N*-methyl-D-aspartate, elicits TTX-insensitive increases in dialysate dopamine (Keefe *et al.*, 1992, 1993) and TTX-insensitive and Ca^{2+}-independent dopamine release *in vitro* (Iravani & Kruk, 1996). Thus, it would appear that if AMPH elicits action potential-independent dopamine efflux *in vivo*, our FSCV approach would have detected it.

Dopamine efflux and action potential-dependent dopamine signalling

Our results with TTX clearly argue against an action potential-independent component of DA efflux contributing to AMPH elevating NAc dopamine. However, AMPH-induced dopamine efflux is voltage sensitive and Na^+ dependent (Khoshbouei *et al.*, 2003; Kahlig *et al.*, 2005). These characteristics suggest that dopamine efflux could be action potential dependent and that TTX prevents this AMPH action *in vivo*. Although we cannot rule out this possibility, it should be noted that there is no direct evidence that action potentials increase AMPH-induced dopamine efflux. Indeed, the voltage sensitivity of efflux was demonstrated in cells expressing the dopamine transporter by depolarizing pulses much longer that the duration of action potentials. AMPH-induced dopamine efflux is also relatively insensitive to depolarizing stimuli in preparations of dopamine terminals. During AMPH-induced dopamine efflux, for example, 15 mM K^+ and electrial stimulation do not evoke further dopamine release in synaptosomes (Bowyer *et al.*, 1987) and slices (Jones *et al.*, 1998), respectively. Moreover, although the uptake of dopamine by the dopamine transporter is similarly voltage sensitive and Na^+ dependent (Amara & Kuhar, 1993), it is insensitive to TTX in spontaneously active dopamine neurons in culture (Prasad & Amara, 2001). The proposed basis of the TTX insensivity is the turnover of the dopamine transporter, which is too slow (0.74/s) to effectively function on the time scale of the firing rate of dopamine neurons (> 5 Hz). TTX does not alter dopamine uptake by synaptosomes (Harris & Baldessarini, 1973), suggesting that it operates by a similar mechanism in native dopamine neurons. As a carrier-mediated process, AMPH-induced dopamine efflux may also be refractory to action potentials.

A channel-like mode of dopamine release mediated by the dopamine transporter has also been described for AMPH (Kahlig *et al.*, 2005). Faster than reverse dopamine transport and supporting the movement of dopamine molecules equivalent to a dopamine vesicle, this non-exocytotic release could support action potential-dependent, AMPH-induced dopamine transients. However, we consider this possibility unlikely for several reasons. First, although channel-like activity is elicited by a depolarizing pulse, it does not appear to be precisely time locked in a way that it would temporally respond to a burst of action potentials and generate a dopamine transient. Second, our *in vivo* results are inconsistent with AMPH depleting dopamine vesicles. Thus, because cytosolic dopamine drives release in channel-like mode, there would appear to be an insufficient source of dopamine to produce the large-amplitude transient. Third, extracellular dopamine inhibits AMPH-induced, channel-like dopamine efflux, which would limit its operation during the successive release events summating to generate a dopamine transient.

Action potential-dependent amphetamine actions

Our results are consistent with action potential-dependent actions of AMPH. Ostensibly, the activation of dopamine transients is incompatible with efflux driven by vesicular depletion, because these phasic signals are dependent on intact vesicular dopamine (Owesson-White *et al.*, 2012). Transient activation has also been reported for other abused drugs, such as cannabinoids, cocaine, ethanol, nicotine and opioids (Cheer *et al.*, 2004, 2007; Aragona *et al.*, 2008; Vander Weele *et al.*, 2014), suggesting a shared action. Indeed, the generation of these phasic dopamine signals is implicated in drug reinforcement (Stuber *et al.*, 2005) and

can produce an addictive phenotype (Pascoli *et al.*, 2015). The present study extends AMPH-induced transient activation in two important ways.

First, RIMO decreased AMPH-induced dopamine transients. Because blocking CB1 receptors also reduces transient activation by cannabinoids, cocaine, nicotine and ethanol (Cheer *et al.*, 2004, 2007), endocannabinoid-mediated activation of phasic dopamine signalling appears to be emerging as a common mechanism in drug reinforcement (Lupica & Riegel, 2005; Parsons & Hurd, 2015). RIMO targeting the NAc is not supported by our findings, demonstrating that electrically evoked dopamine signals and dopamine uptake were unaltered by CB1 receptor blockade, in agreement with previous work (Szabo *et al.*, 1999; Oleson *et al.*, 2012), as were effects of AMPH on these measures. Consistent with the VTA as a likely target, intra-VTA RIMO injection reduces cocaine-induced transient activation (Wang *et al.*, 2015), similar to intravenous RIMO administration (Cheer *et al.*, 2007), and CB1 receptor drugs modify VTA dopamine neuron electrophysiology measured in slices (Riegel & Lupica, 2004; Wang *et al.*, 2015). Dopamine neurons also do not express CB1 receptors (Julian *et al.*, 2003), suggesting that RIMO is acting indirectly on dopamine signalling. Consistent with this idea, endocannabinoids are synthesized and released by dopamine neurons as retrograde messengers that inhibit afferent input via CB1 receptor binding on terminals (Riegel & Lupica, 2004; Matyas *et al.*, 2008). CB1 receptor-mediated suppression of GABA inputs is hypothesized to allow addictive drugs or reward-associated stimuli to disinhibit dopamine neurons projecting to the NAc (Lupica & Riegel, 2005; Oleson *et al.*, 2012). Because RIMO concurrently reduces reward seeking and dopamine transients evoked by reward-predicting cues (Oleson *et al.*, 2012), diminished phasic dopamine signalling may underlie the suppression of drug reward, reinforcement and relapse by CB1 receptor antagonists (Lupica & Riegel, 2005; De Vries & Schoffelmeer, 2005; Fattore *et al.*, 2007). Thus, CB1 receptors are an attractive target for treating drug abuse and addiction.

Second, new insight is obtained by resolving direct and indirect effects of AMPH on dopamine transients. Path analysis confirmed that AMPH increases transient frequency, amplitude and duration, but uniquely demonstrated that frequency and amplitude are increased independently. These relationships support a novel model of AMPH action. Rather than evoke action potential-independent dopamine efflux, the most parsimonious explanation based on our findings is that AMPH elicits dopamine transients by generating burst firing of dopamine neurons facilitated by endocannabinoids. This action supports the hypothesis that abused drugs mimic natural rewards by eliciting transients *de novo* but to a greater extent, leading to hijacking of reward circuits and overlearning of cues predicting drug availability (Hyman *et al.*, 2006; Covey *et al.*, 2014) and extends this hypothesis by identifying endocannabinoids as the linchpin in transient generation. AMPH is also proposed to increase transient amplitude by enhancing intraburst properties and increasing exocytotic dopamine release, and to elevate NAc dopamine by inhibiting dopamine uptake, leading to the accumulation of successive transients made more numerous, larger and wider by AMPH.

Selection of rimonabant to block cannabinoid type 1 receptors

We selected RIMO to investigate the role of endocannabinoids in AMPH-induced elevations in NAc dopamine, because this CB1 receptor antagonist has been used to assess similar actions of cocaine, ethanol, nicotine and cannabinoids, and to support the hypothesis that endocannabioids faciliate the activation of dopamine transients by broad classes of abused drugs (Cheer *et al.*, 2004, 2007; Wang *et al.*, 2015). RIMO therefore enabled us to directly compare the present results with previous work and demonstrate a similar regulatory mechanism for AMPH-evoked elevations in NAc dopamine. Moreover, the effects of RIMO on dopamine signalling associated with abused drugs and reward-related stimuli (Oleson *et al.*, 2012) are consistent with other pharmacological or genetic manipulations of CB1 receptor function that alter dopamine-dependent, brain reinforcement mechanisms (Lupica & Riegel, 2005; Covey *et al.*, 2015; Parsons & Hurd, 2015).

The selectivity of RIMO can be questioned based on its antagonism of mu-opioid receptors (Seely *et al.*, 2012; Zador *et al.*, 2012). Although we cannot rule a contribution of these receptors, our findings are more consistent with RIMO acting on CB1 receptors. For example, RIMO acts in the VTA and not the striatum to alter dopamine signalling and does not alter the baseline activity of dopamine neurons (Szabo *et al.*, 1999; Cheer *et al.*, 2004, 2007; Oleson *et al.*, 2012; Wang *et al.*, 2015). In contrast, mu-opioid drugs target both regions and tonically alter dopamine signalling (Leone *et al.*, 1991; Spanagel *et al.*, 1992; Devine *et al.*, 1993; Dourmap *et al.*, 1997; Mathon *et al.*, 2006). Because RIMO did not act on dopamine terminals and did not alter the baseline characteristics of dopamine transients, our results thus suggest a CB1 receptor mechanism. Also consistent with blocking CB1 receptors in the present study, RIMO has a >350-fold higher affinity for the CB1 receptor compared with the mu-opioid receptor, and, although it partially blocks morphine-induced analgesia *in vivo*, the dose used to achieve this effect is 30- fold higher than that used here (Seely *et al.*, 2012). Taken together, these findings suggest that blockade of CB1 receptors is the predominate action of RIMO in reducing AMPH-induced elevations in NAc dopamine.

Conclusion

The present findings are consistent with AMPH elevating NAc dopamine by a complex mechanism consisting of action potential generation, endocannabinoid-mediated activation of phasic dopamine signalling, enhanced exocytotic dopamine release and dopamine uptake inhibition, but not by eliciting action potential-independent dopamine efflux.

Acknowledgments

This work was supported by the National Institute on Drug Abuse (DA 024036 and DA 036331 to P.A.G.; EBO 14539 to J.F.C.).

Abbreviations

aCSF	artificial cerebrospinal fluid
AMPH	amphetamine
CB1	cannabinoid type 1

FSCV	fast-scan cyclic voltammetry
NAc	nucleus accumbens
RIMO	rimonabant
TTX	tetrodotoxin
VEH	vehicle
VTA	ventral tegmental area

References

Amara SG, Kuhar MJ. Neurotransmitter transporters: recent progress. Annu Rev Neurosci. 1993; 16:73–93. [PubMed: 8096377]

Anderson, DR. Model Based Inference in the Life Sciences. A Primer on Evidence. Springer Science Business Media; New York: 2008.

Aragona BJ, Cleaveland NA, Stuber GD, Day JJ, Carelli RM, Wightman RM. Preferential enhancement of dopamine transmission within the nucleus accumbens shell by cocaine is attributable to a direct increase in phasic dopamine release events. J Neurosci. 2008; 28:8821–8831. [PubMed: 18753384]

Avelar AJ, Juliano SA, Garris PA. Amphetamine augments vesicular dopamine release in the dorsal and ventral striatum through different mechanisms. J Neurochem. 2013; 125:373–385. [PubMed: 23406303]

Bales JW, Wagner AK, Kline AE, Dixon CE. Persistent cognitive dysfunction after traumatic brain injury: a dopamine hypothesis. Neurosci Biobehav R. 2009; 33:981–1003.

Benwell ME, Balfour DJ, Lucchi HM. Influence of tetrodotoxin and calcium on changes in extracellular dopamine levels evoked by systemic nicotine. Psychopharmacology. 1993; 112:467–474. [PubMed: 7871059]

Borland LM, Michael AC. Voltammetric study of the control of striatal dopamine release by glutamate. J Neurochem. 2004; 91:220–229. [PubMed: 15379902]

Bowyer JF, Masserano JM, Weiner N. Inhibitory effects of amphetamine on potassium-stimulated release of [3H]dopamine from striatal slices and synaptosomes. J Pharmacol Exp Ther. 1987; 240:177–186. [PubMed: 3100768]

Browman KE, Badiani A, Robinson TE. Modulatory effect of environmental stimuli on the susceptibility to amphetamine sensitization: a dose-effect study in rats. J Pharmacol Exp Ther. 1998; 287:1007–1014. [PubMed: 9864286]

Bunney BS, Walters JR, Roth RH, Aghajanian GK. Dopaminergic neurons: effect of antipsychotic drugs and amphetamine on single cell activity. J Pharmacol Exp Ther. 1973; 185:560–571. [PubMed: 4576427]

Calipari ES, Ferris MJ, Zimmer BA, Roberts DC, Jones SR. Temporal pattern of cocaine intake determines tolerance vs sensitization of cocaine effects at the dopamine transporter. Neuropsychopharmacology. 2013; 38:2385–2392. [PubMed: 23719505]

Cheer JF, Wassum KM, Heien ML, Phillips PE, Wightman RM. Cannabinoids enhance subsecond dopamine release in the nucleus accumbens of awake rats. J Neurosci. 2004; 24:4393–4400. [PubMed: 15128853]

Cheer JF, Heien ML, Garris PA, Carelli RM, Wightman RM. Simultaneous electrochemical and single-unit recordings in the nucleus accumbens reveal GABA-mediated responses: implications for intracranial self-stimulation. Proc Natl Acad Sci USA. 2005; 102:19150–19155. [PubMed: 16380429]

Cheer JF, Wassum KM, Sombers LA, Heien ML, Ariansen JL, Aragona BJ, Phillips PE, Wightman RM. Phasic dopamine release evoked by abused substances requires cannabinoid receptor activation. J Neurosci. 2007; 27:791–795. [PubMed: 17251418]

Covey DP, Juliano SA, Garris PA. Amphetamine elicits opposing actions on readily releasable and reserve pools for dopamine. PLoS One. 2013; 8:e60763. [PubMed: 23671560]

Covey DP, Roitman MF, Garris PA. Illicit dopamine transients: reconciling actions of abused drugs. Trends Neurosci. 2014; 37:200–210. [PubMed: 24656971]

Covey DP, Wenzel JM, Cheer JF. Cannabinoid modulation of drug reward and the implications of marijuana legalization. Brain Res. 2015; 1628:233–243. [PubMed: 25463025]

Daberkow DP, Brown HD, Bunner KD, Kraniotis SA, Doellman MA, Ragozzino ME, Garris PA, Roitman MF. Amphetamine paradoxically augments exocytotic dopamine release and phasic dopamine signals. J Neurosci. 2013; 33:452–463. [PubMed: 23303926]

De Vries TJ, Schoffelmeer AN. Cannabinoid CB1 receptors control conditioned drug seeking. Trends Pharmacol Sci. 2005; 26:420–426. [PubMed: 15992935]

Devine DP, Leone P, Wise RA. Mesolimbic dopamine neurotransmission is increased by administration of mu-opioid receptor antagonists. Eur J Pharmacol. 1993; 243:55–64. [PubMed: 7902813]

Di Chiara CG, Imperato A. Drugs abused by humans preferentially increase synaptic dopamine concentrations in the mesolimbic system of freely moving rats. Proc Natl Acad Sci USA. 1988; 85:5274–5278. [PubMed: 2899326]

Dourmap N, Clero E, Costentin J. Involvement of cholinergic neurons in the release of dopamine elicited by stimulation of mu-opioid receptors in striatum. Brain Res. 1997; 749:295–300. [PubMed: 9138730]

Fattore L, Fadda P, Fratta W. Endocannabinoid regulation of relapse mechanisms. Pharmacol Res. 2007; 56:418–427. [PubMed: 17936008]

Fischer JF, Cho AK. Chemical release of dopamine from striatal homogenates: evidence for an exchange diffusion model. J Pharmacol Exp Ther. 1979; 208:203–209. [PubMed: 762652]

Forray A, Sofuoglu M. Future pharmacological treatments for substance use disorders. Br J Clin Pharmacol. 2014; 77:382–400. [PubMed: 23039267]

Freund N, Manns M, Rose J. A method for the evaluation of intracranial tetrodotoxin injections. J Neurosci Meth. 2010; 186:25–28.

Harris JE, Baldessarini RJ. The uptake of (3H)dopamine by homogenates of rat corpus striatum: effects of cations. Life Sci. 1973; 13:303–312. [PubMed: 4127606]

Hamid AA, Pettibone JR, Mabrouk OS, Hetrick VL, Schmidt R, Vander Weele CM, Kennedy RT, Aragona BJ, Berke JD. Mesolimbic dopamine signals the value of work. Nat Neurosci. 2016; 19:117–126. [PubMed: 26595651]

Heien ML, Phillips PE, Stuber GD, Seipel AT, Wightman RM. Overoxidation of carbon-fiber microelectrodes enhances dopamine adsorption and increases sensitivity. Analyst. 2003; 128:1413–1419. [PubMed: 14737224]

Heien ML, Khan AS, Ariansen JL, Cheer JF, Phillips PE, Wassum KM, Wightman RM. Real-time measurement of dopamine fluctuations after cocaine in the brain of behaving rats. Proc Natl Acad Sci USA. 2005; 102:10023–10028. [PubMed: 16006505]

Hermans A, Keithley RB, Kita JM, Sombers LA, Wightman RM. Dopamine detection with fast-scan cyclic voltammetry used with analog background subtraction. Anal Chem. 2008; 80:4040–4048. [PubMed: 18433146]

Howell LL, Kimmel HL. Monoamine transporters and psychostimulant addiction. Biochem Pharmacol. 2008; 75:196–217. [PubMed: 17825265]

Hyman SE, Malenka RC, Nestler EJ. Neural mechanisms of addiction: the role of reward-related learning and memory. Annu Rev Neurosci. 2006; 29:565–598. [PubMed: 16776597]

Iravani MM, Kruk ZL. Effects of amphetamine on carriermediated and electrically stimulated dopamine release in slices of rat caudate putamen and nucleus accumbens. J Neurochem. 1995; 64:1161–1168. [PubMed: 7861147]

Iravani MM, Kruk ZL. Real-time effects of *N*-methyl-D-aspartic acid on dopamine release in slices of rat caudate putamen: a study using fast cyclic voltammetry. J Neurochem. 1996; 66:1076–1085. [PubMed: 8769869]

Jaquins-Gerstl A, Michael AC. A review of the effects of FSCV and microdialysis measurements on dopamine release in the surrounding tissue. Analyst. 2015; 140:3696–3708. [PubMed: 25876757]

Jones SR, Gainetdinov RR, Wightman RM, Caron MG. Mechanisms of amphetamine action revealed in mice lacking the dopamine transporter. J Neurosci. 1998; 18:1979–1986. [PubMed: 9482784]

Julian MD, Martin AB, Cuellar B, Rodriguez De Fonseca F, Navarro M, Moratalla R, Garcia-Segura LM. Neuroanatomical relationship between type 1 cannabinoid receptors and dopaminergic systems in the rat basal ganglia. Neuroscience. 2003; 119:309–318. [PubMed: 12763090]

Kahlig KM, Binda F, Khoshbouei H, Blakely RD, McMahon DG, Javitch JA, Galli A. Amphetamine induces dopamine efflux through a dopamine transporter channel. Proc Natl Acad Sci USA. 2005; 102:3495–3500. [PubMed: 15728379]

Keefe KA, Zigmond MJ, Abercrombie ED. Extracellular dopamine in striatum: influence of nerve impulse activity in medial forebrain bundle and local glutamatergic input. Neuroscience. 1992; 47:325–332. [PubMed: 1353620]

Keefe KA, Zigmond MJ, Abercrombie ED. In vivo regulation of extracellular dopamine in the neostriatum: influence of impulse activity and local excitatory amino acids. J Neural Transm Gen. 1993; 91:223–240.

Khoshbouei H, Wang H, Lechleiter JD, Javitch JA, Galli A. Amphetamine-induced dopamine efflux. A voltage-sensitive and intracellular Na+-dependent mechanism. J Biol Chem. 2003; 278:12070–12077. [PubMed: 12556446]

Kuczenski, R. Biochemical actions of amphetamine and other stimulants. In: Creese, I., editor. Stimulants: Neurochemical, Behavioral and Clinical Perspectives. Raven Press; New York: 1983. p. 31-61.

Kuczenski, R., Segal, DS. Neurochemistry of Amphetamine. In: Cho, A., Segal, DS., editors. Amphetamine and its Analogs. Academic Press; San Diego, CA: 1994. p. 81-113.

Kuczenski R, Segal DS, Aizenstein M. Amphetamine, cocaine, and fencamfamine: relationship between locomotor and stereotypy response profiles and caudate and accumbens dopamine dynamics. J Neurosci. 1991; 11:2703–2712. [PubMed: 1715389]

Kuczenski R, Melega WP, Cho AK, Segal DS. Extracellular dopamine and amphetamine after systemic amphetamine administration: comparison to the behavioral response. J Pharmacol Exp Ther. 1997; 282:591–596. [PubMed: 9262319]

Leone P, Pocock D, Wise RA. Morphine-dopamine interaction: ventral tegmental morphine increases nucleus accumbens dopamine release. Pharmacol Biochem Be. 1991; 39:469–472.

Lupica CR, Riegel AC. Endocannabinoid release from midbrain dopamine neurons: a potential substrate for cannabinoid receptor antagonist treatment of addiction. Neuropharmacology. 2005; 48:1105–1116. [PubMed: 15878779]

Mathon DS, Vanderschuren LJ, Ramakers GM. Reduced psychostimulant effects on dopamine dynamics in the nucleus accumbens of mu-opioid receptor knockout mice. Neuroscience. 2006; 141:1679–1684. [PubMed: 16777349]

Matyas F, Urban GM, Watanabe M, Mackie K, Zimmer A, Freund TF, Katona I. Identification of the sites of 2-arachidonoylglycerol synthesis and action imply retrograde endocannabinoid signaling at both GABAergic and glutamatergic synapses in the ventral tegmental area. Neuropharmacology. 2008; 54:95–107. [PubMed: 17655884]

Michael DJ, Joseph JD, Kilpatrick MR, Travis ER, Wightman RM. Improving data acquisition for fast-scan cyclic voltammetry. Anal Chem. 1999; 71:3941–3947. [PubMed: 10500480]

Milesi-Hallé A, McMillian DE, Laurenzana EM, Byrnes-Blake KA, Owens SM. Sex differences in (+)-amphetamine- and (+)-metham-phetamine-induced behavioral response in male and female Sprague-Dawley rats. Pharmacol Biochem Be. 2007; 86:140–149.

Mitchell, RJ. Path analysis: pollination. In: Scheiner, SM., Gurevitch, J., editors. Design and Analysis of Ecological Experiments. Oxford University Press; Oxford, UK: 2001. p. 217-234.

Nestler EJ. Is there a common molecular pathway for addiction? Nat Neurosci. 2005; 8:1445–1449. [PubMed: 16251986]

Nomikos GG, Damsma G, Wenkstern D, Fibiger HC. In vivo characterization of locally applied dopamine uptake inhibitors by striatal microdialysis. Synapse. 1990; 6:106–112. [PubMed: 1697988]

Oleson EB, Beckert MV, Morra JT, Lansink CS, Cachope R, Abdullah RA, Loriaux AL, Schetters D, et al. Endocannabinoids shape accumbal encoding of cue-motivated behavior via CB1 receptor activation in the ventral tegmentum. Neuron. 2012; 73:360–373. [PubMed: 22284189]

Omiatek DM, Dong Y, Heien ML, Ewing AG. Only a fraction of quantal content is released during exocytosis as revealed by electrochemical cytometry of secretory vesicles. ACS Chem Neurosci. 2010; 1:234–245. [PubMed: 20368748]

Owesson-White CA, Roitman MF, Sombers LA, Belle AM, Keithley RB, Peele JL, Carelli RM, Wightman RM. Sources contributing to the averaged extracellular concentration of dopamine in the nucleus accumbens. J Neurochem. 2012; 121:252–262. [PubMed: 22296263]

Parsons LH, Hurd YL. Endocannabinoid signalling in reward and addiction. Nat Rev Neurosci. 2015; 16:579–594. [PubMed: 26373473]

Pascoli V, Terrier J, Hiver A, Lüscher C. Sufficiency of mesolimbic dopamine neuron stimulation for the progresssion to addiction. Neuron. 2015; 88:1054–1066. [PubMed: 26586182]

Patel J, Mooslehner KA, Chan PM, Emson PC, Stamford JA. Presynaptic control of striatal dopamine neurotransmission in adult vesicular monoamine transporter 2 (VMAT2) mutant mice. J Neurochem. 2003; 85:898–910. [PubMed: 12716422]

Paxinos, G., Watson, C. The Rat Brain in Stereotaxic Coordinates. 4. Academic; San Diego: 1998.

Pickens R, Harris WC. Self-administration of D-amphetamine by rats. Psychopharmacologia. 1968; 12:158–163. [PubMed: 5657050]

Prasad BM, Amara SG. The dopamine transporter in mesencephalic cultures is refractory to physiological changes in membrane voltage. J Neurosci. 2001; 21:7561–7567. [PubMed: 11567046]

Ramsson ES, Howard CD, Covey DP, Garris PA. High doses of amphetamine augment, rather than disrupt, exocytotic dopamine release in the dorsal and ventral striatum of the anesthetized rat. J Neurochem. 2011; 119:1162–1172. [PubMed: 21806614]

Riegel AC, Lupica CR. Independent presynaptic and postsynaptic mechanisms regulate endocannabinoid signaling at multiple synapses in the ventral tegmental area. J Neurosci. 2004; 24:11070–11078. [PubMed: 15590923]

Robinson DL, Hermans A, Seipel AT, Wightman RM. Monitoring rapid chemical communication in the brain. Chem Rev. 2008; 108:2554–2584. [PubMed: 18576692]

Schmitz Y, Lee CJ, Schmauss C, Gonon F, Sulzer D. Amphetamine distorts stimulation-dependent dopamine overflow: effects on D2 autoreceptors, transporters, and synaptic vesicle stores. J Neurosci. 2001; 21:5916–5924. [PubMed: 11487614]

Seely KA, Brents LK, Franks LN, Rajasekaran M, Zimmerman SM, Fantegrossi WE, Prather PL. AM-251 and rimonabant act as direct antagonists at mu-opioid receptors: implications for opioid/cannabinoid interaction studies. Neuropharmacology. 2012; 63:905–915. [PubMed: 22771770]

Seiden LS, Sabol KE, Ricaurte GA. Amphetamine: effects on catecholamine systems and behavior. Annu Rev Pharmacol Toxicol. 1993; 33:639–677. [PubMed: 8494354]

Shi WX, Pun CL, Zhang XX, Jones MD, Bunney BS. Dual effects of D-amphetamine on dopamine neurons mediated by dopamine and nondopamine receptors. J Neurosci. 2000; 20:3504–3511. [PubMed: 10777813]

Shi WX, Pun CL, Zhou Y. Psychostimulants induce low-frequency oscillations in the firing activity of dopamine neurons. Neuropsychopharmacology. 2004; 29:2160–2167. [PubMed: 15257309]

Siciliano CA, Calipari ES, Ferris MJ, Jones SR. Biphasic mechanisms of amphetamine action at the dopamine terminal. J Neurosci. 2014; 34:5575–5582. [PubMed: 24741047]

Sombers LA, Beyene M, Carelli RM, Wightman RM. Synaptic overflow of dopamine in the nucleus accumbens arises from neuronal activity in the ventral tegmental area. J Neurosci. 2009; 29:1735–1742. [PubMed: 19211880]

Spanagel R, Herz A, Shippenberg TS. Opposing tonically active endogenous opioid systems modulate the mesolimbic dopaminergic pathway. Proc Natl Acad Sci USA. 1992; 89:2046–2050. [PubMed: 1347943]

Steinberg EE, Boivin JR, Saunders BT, Witten IB, Deisseroth K, Janak PH. Positive reinforcement mediated by midbrain dopamine neurons requires D1 and D2 receptor activation in the nucleus accumbens. PLoS One. 2014; 9:e94771. [PubMed: 24733061]

Stoops WW, Rush CR. Combination pharmacotherapies for stimulant use disorder: a review of clinical findings and recommendations for future research. Expert Rev Clin Pharmacol. 2014; 7:363–374. [PubMed: 24716825]

Stuber GD, Roitman MF, Phillips PE, Carelli RM, Wightman RM. Rapid dopamine signaling in the nucleus accumbens during contingent and noncontingent cocaine administration. Neuropsychopharmacology. 2005; 30:853–863. [PubMed: 15549053]

Sulzer D. How addictive drugs disrupt presynaptic dopamine neurotransmission. Neuron. 2011; 69:628–649. [PubMed: 21338876]

Sulzer D, Sonders MS, Poulsen NW, Galli A. Mechanisms of neurotransmitter release by amphetamines: a review. Prog Neurobiol. 2005; 75:406–433. [PubMed: 15955613]

Szabo B, Muller T, Koch H. Effects of cannabinoids on dopamine release in the corpus striatum and the nucleus accumbens in vitro. J Neurochem. 1999; 73:1084–1089. [PubMed: 10461898]

UNODC. United Nations Office on Drugs and Crime: World Drug Report 2014. 2014.

Vander Weele CM, Porter-Stransky KA, Mabrouk OS, Lovic V, Singer BF, Kennedy RT, Aragona BJ. Rapid dopamine transmission within the nucleus accumbens: dramatic difference between morphine and oxycodone delivery. Eur J Neurosci. 2014; 40:3041–3054. [PubMed: 25208732]

Ventura R, Alcaro A, Mandolesi L, Puglisi-Allegra S. In vivo evidence that genetic background controls impulse-dependent dopamine release induced by amphetamine in the nucleus accumbens. J Neurochem. 2004; 89:494–502. [PubMed: 15056292]

Wang H, Treadway T, Covey DP, Cheer JF, Lupica CR. Cocaine-induced endocannabinoid mobilization in the ventral tegmental area. Cell Rep. 2015; 12:1997–2008. [PubMed: 26365195]

Westerink BH, Tuntler J, Damsma G, Rollema H, De Vries JB. The use of tetrodotoxin for the characterization of drug-enhanced dopamine release in conscious rats studied by brain dialysis. Naunyn Schmiedebergs Arch Pharmacol. 1987; 336:502–507. [PubMed: 3501841]

Wiedemann DJ, Basse-Tomusk A, Wilson RL, Rebec GV, Wightman RM. Interference by DOPAC and ascorbate during attempts to measure drug-induced changes in neostriatal dopamine with Nafioncoated, carbon-fiber electrodes. J Neurosci Method. 1990; 35:9–18.

Wightman RM, Heien ML, Wassum KM, Sombers LA, Aragona BJ, Khan AS, Ariansen JL, Cheer JF, et al. Dopamine release is heterogeneous within microenvironments of the rat nucleus accumbens. Eur J Neurosci. 2007; 26:2046–2054. [PubMed: 17868375]

Yokel RA, Pickens R. Self-administration of optical isomers of amphetamine and methylamphetamine by rats. J Pharmacol Exp Ther. 1973; 187:27–33. [PubMed: 4795731]

Yorgason JT, Espana RA, Jones SR. Demon voltammetry and analysis software: analysis of cocaine-induced alterations in dopamine signaling using multiple kinetic measures. J Neurosci Meth. 2011; 202:158–164.

Zador F, Otvos F, Benyhe S, Zimmer A, Paldy E. Inhibition of forebrain mu-opioid receptor signaling by low concentrations of rimonabant does not require cannabinoid receptors and directly involves muopioid receptors. Neurochem Int. 2012; 61:378–388. [PubMed: 22613132]

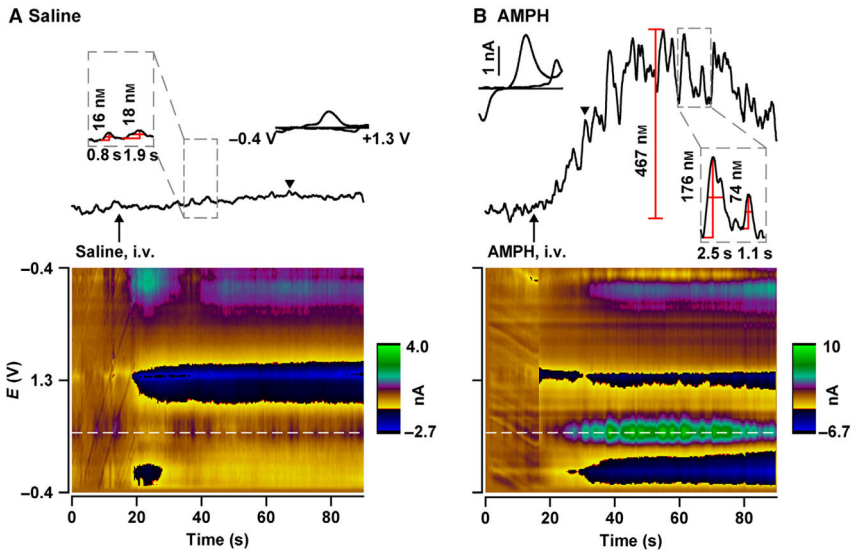

Fig. 1.

AMPH elevates NAc dopamine measured by FSCV. Representative recordings following intravenously administered saline (A) and AMPH (B). Arrow indicates drug injection. Individual dopamine transients, highlighted within dashed boxes, were analysed for amplitude (peak), duration (width at half-maximal amplitude) and frequency (inverse of inter-transient interval). Amplitudes and duration are shown above and below individual transients, respectively. The maximal increase in dopamine concentration relative to 0 s (B, vertical red line) was used to average dopamine concentration across recording epochs. Signals were electrochemically verified as dopamine by plotting the oxidative and reductive currents vs. the applied potential to form individual background-subtracted cyclic voltammograms (inset: black triangle indicates time point when cyclic voltammogram was derived). Colour plots below each trace display background-subtracted cyclic voltammograms sequentially in time (*x*-axis, time; *y*-axis, applied potential; *z*-axis or false colour, measured current). The dopamine record shown above was determined by measuring current at the peak dopamine oxidative potential (~0.65 V), highlighted by the horizontal dashed white line in the colour plot, and converting to concentration.

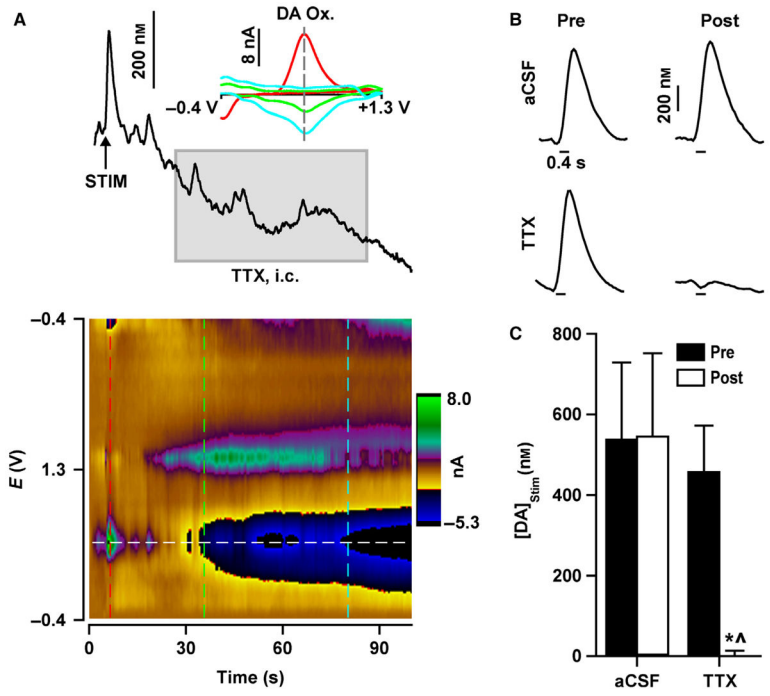

Fig. 2.

TTX abolishes electrically evoked dopamine signals. (A) Representative trace during an intracranial TTX infusion [grey box; TTX, intracranial (i.c.)] into the VTA. Electrical stimulation (STIM; vertical arrow) applied to the VTA prior to TTX elicited dopamine signals mimicking naturally occurring dopamine transients. TTX infusion caused a decrease in basal dopamine that tracks the change in current determined at the dopamine oxidative potential (DA Ox.), as shown by individual background-subtracted cyclic voltammograms (inset) measured at different time points (vertical dashed lines on colour plot). Similar dopamine decreases were also evident in the colour plot (horizontal dashed white line). (B) Representative electrically evoked dopamine signals (stimulation indicated by horizontal line under traces) before (Pre) and after (Post) aCSF or TTX infusion. (C) Maximal concentration of electrically evoked dopamine ($[DA]_{Stim}$) was abolished by TTX but unaffected by aCSF. Data are expressed as mean + SEM. $*P < 0.01$ vs. Pre (within-group comparisons); $\wedge P < 0.01$ vs. aCSF (between-group comparisons).

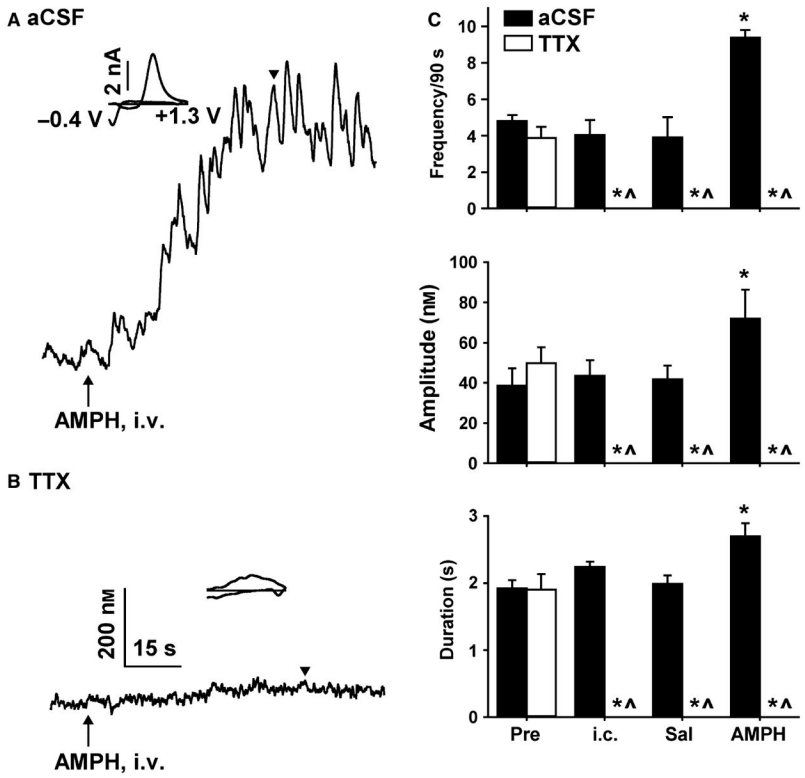

Fig. 3.

TTX abolishes the AMPH-induced activation of dopamine transients. AMPH-induced dopamine elevations following intra-VTA infusions of aCSF (A) and TTX (B) in representative recordings. Black triangle indicates time point when individual background-subtracted cyclic voltammograms were derived (insets). (C) Transient frequency (top), amplitude (middle) and duration (bottom) at baseline (Pre), following intra-cranial (i.c.) infusions, intravenous saline (Sal), and intravenous AMPH. All measures were abolished by TTX. Data are expressed as mean + SEM. *$P < 0.001$ vs. Pre (within-group comparison); ^$P < 0.001$ vs. aCSF (between-group comparison).

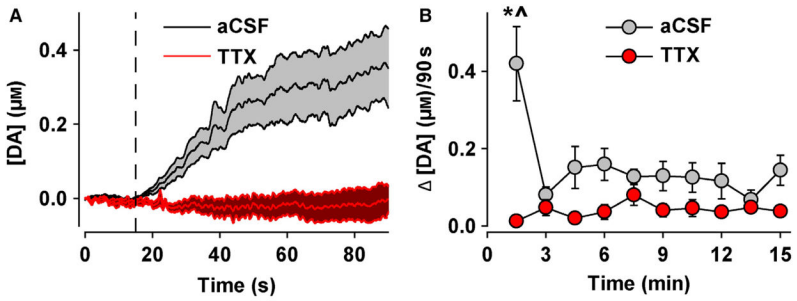

Fig. 4.

TTX abolishes AMPH-induced elevations in the NAc. (A) Dopamine concentration ([DA]) plotted with time during the first 90 s epoch. Either aCSF or TTX was infused into the VTA at the vertical dashed line. (B) Change in the dopamine concentration (Δ[DA]) within each 90 s epoch and plotted with time. Data are expressed as mean ± SEM. *$P < 0.001$ vs. TTX (between-group comparisons); ^$P < 0.001$ vs. aCSF (within-group comparisons).

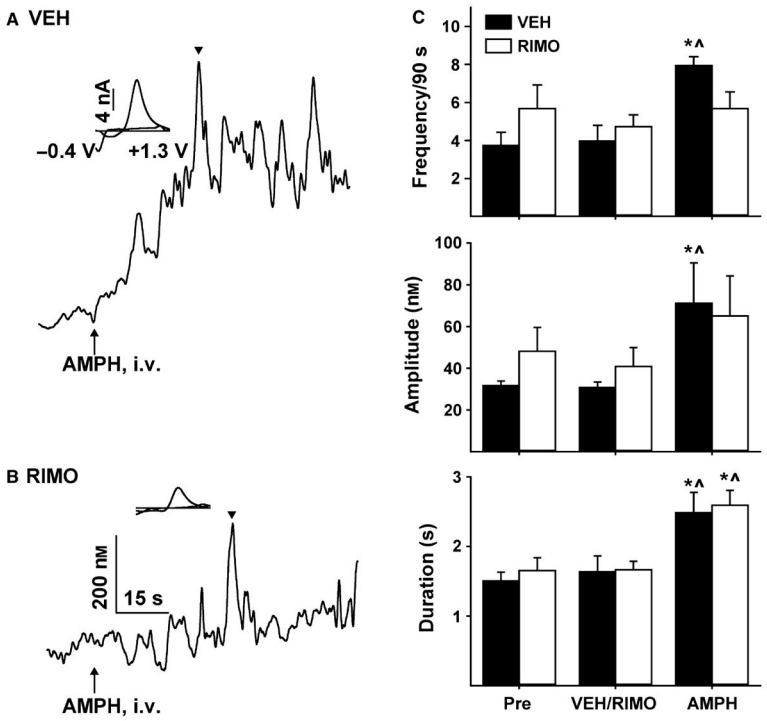

Fig. 5.

RIMO attenuates the AMPH-induced activation of dopamine transients. AMPH-induced dopamine elevations following intravenous administration of VEH (A) and RIMO (B) in representative recordings. Black triangle indicates time point when individual background-subtracted cyclic voltammograms were derived (insets). (C) RIMO prevented AMPH-induced increases in transient frequency (top) and amplitude (middle), but not duration (bottom). Data are expressed as mean + SEM. *$P < 0.01$ vs. baseline (Pre); ^$P < 0.01$ vs. VEH/RIMO (both within-group comparisons).

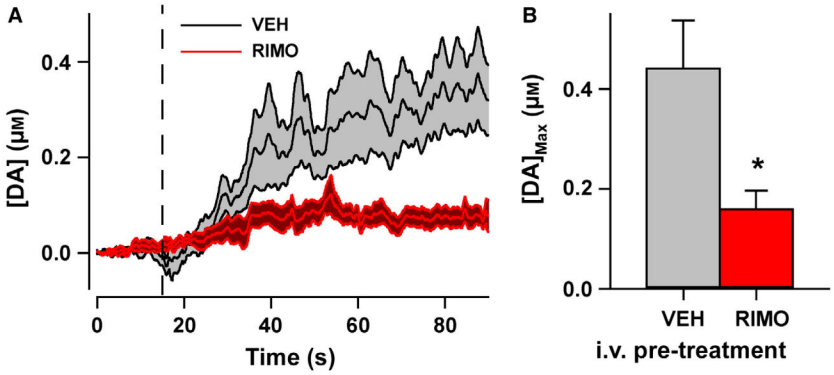

Fig. 6.

RIMO attenuates AMPH-induced elevations in NAc. (A) Dopamine concentrations ([DA]) during the first 90 s epoch. VEH or RIMO was administered intravenously at the vertical dashed line. (B) Change in the maximal dopamine concentration ($[DA]_{Max}$). Data are expressed as mean + SEM. *$P < 0.01$ vs. VEH.

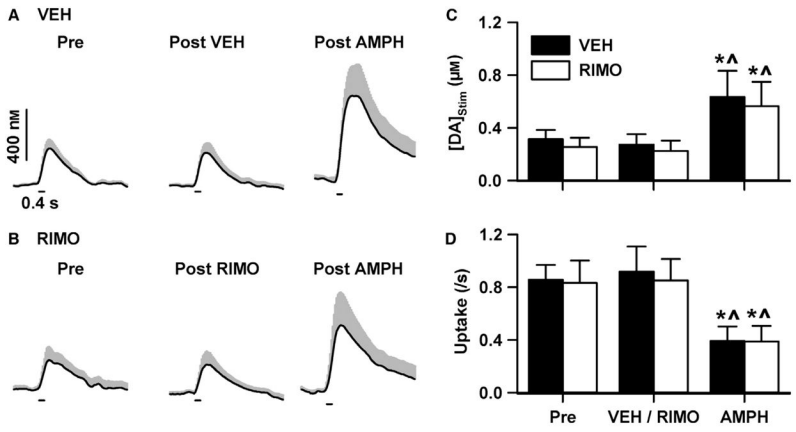

Fig. 7.

RIMO does not act pre-synaptically on dopamine terminals. Electrically evoked dopamine signals recorded in VEH-treated (A) and RIMO-treated (B) animals. Dark line is mean and gray area is SEM. Electrical stimulation of the VTA was applied at the horizontal line. Pre, before VEH or RIMO administration; Post VEH and Post RIMO, after VEH and RIMO administration, respectively; Post AMPH, after AMPH administration. VEH and RIMO did not alter the maximal concentration of electrically evoked dopamine ($[DA]_{Stim}$) (C) or dopamine uptake (D). Data are expressed as mean + SEM. *$P < 0.05$ vs. Pre; ^$P < 0.05$ vs. VEH/RIMO (both within-group comparisons).

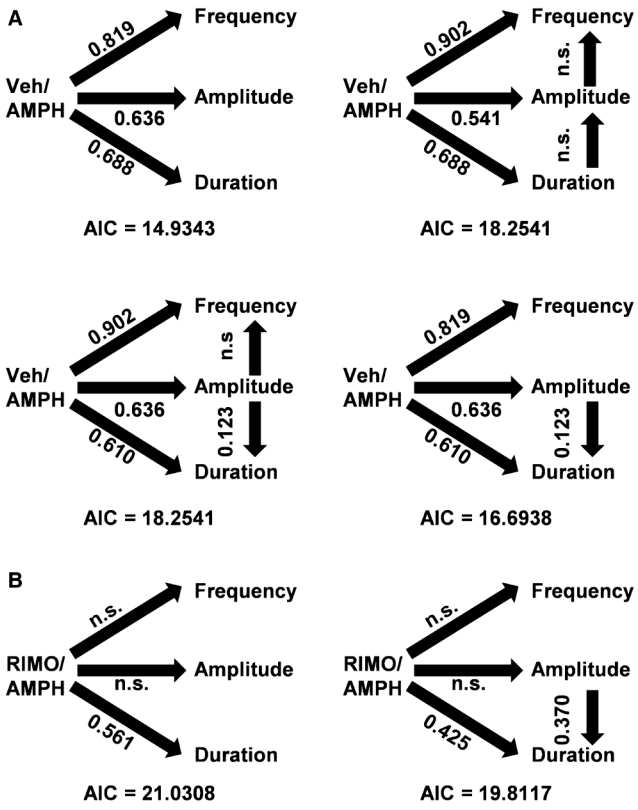

Fig. 8.

Path analysis of the regulation of dopamine transients. (A) Models of AMPH effects. (B) Models of RIMO modulation of AMPH effects. Arrows demarcate the direct effects analysed in each model. Significant path coefficients are given above arrows. AIC, Akaike information criteria; n.s., not significant.